文章编号：1006-9941(2018)01-0059-07

Ab Initio Molecular Dynamics Studies on the Decomposition Mechanisms of CL-20 Crystal under Extreme Conditions

XIANG Dong[1], **WU Qiong**[2], **ZHU Wei-hua**[1]

(1. *Institute for Computation in Molecular and Materials Science, School of Chemical Engineering, Nanjing University of Science and Technology, Nanjing* 210094, *China*; 2. *School of Materials Science and Engineering, Nanjing Institute of Technology, Nanjing* 211167, *China*)

Abstract: Ab initio molecular dynamics simulations were used to study the decomposition mechanism of 2,4,6,8,10,12-hexanitro-2,4,6,8,10,12-hexaazaisowurtzitane(CL-20) crystal, an excellent high energy density cage compound, under extreme conditions. It is found that the initiation and subsequent decomposition mechanisms of the CL-20 crystal are diverse at different conditions, and CL-20 is sensitive to both high temperature and pressure. Comparing the numbers of corresponding main products, it is found that the high pressure decelerates the decomposition. While, the appearance of special intermediates *R*-C_xO_y(x>2, y>5) indicates that the high pressure makes the decomposition much more complex. Among these intermediates, C_3O_6 is proved to be a high energy density compound.

Key words: Ab initio molecular dynamics, 2,4,6,8,10,12-hexanitro-2,4,6,8,10,12-hexaazaisowurtzitane(CL-20), decomposition, extreme conditions

CLC number: TJ55; O64 **Document code**: A **DOI**: 10.11943/j.issn.1006-9941.2018.01.007

1 Introduction

The initial chemical events in the decompositions of condensed phase explosives under extreme conditions are very important to understand their complicated behaviors, to control their risk during usage and storage, and to develop new high-energy explosives[1]. 2,4,6,8,10,12-hexanitro-2,4,6,8,10,12-hexaazaisowurtzitane(CL-20), one of the most powerful high explosives, has a relatively high ambient temperature density of 2.04 g·cm^{-3}[4]. CL-20 has a high heat of formation[2] and detonation performance of D=9.6 km·s^{-1} and p=43 GPa with an isowurzitane cage structure and several nitramine groups[3]. The toxicity and potential carcinogenicity of CL-20 and its transformation products have led to concern about its fate in the environment and potential harm to human health. Major transformation processes of this compound in the environment occur at moderate but variable rates conditions[5]. It is thus very necessary to study the decomposition mechanisms of CL-20 under extreme conditions.

However, it is difficult to investigate many aspects of their reactivity with chemical experimental techniques. Molecular simulations offer risk-free and relatively accurate ways to study their behavior. Several studies[6-10] using ab initio molecular dynamics (AIMD) to study the details of the gas phase unimolecular and bimolecular reaction decompositions of the explosives at realistic reaction temperatures and pressures have seen tremendous progress in confirming and interpreting experimental observables. Recently, a computational DFT study[11] on the unimolecular decompositions of CL-20 showed that there are several types of reaction mechanisms for this process: an N—N bond homolytic cleavage to form the NO_2 group, HONO elimination, the breaking of C—C and C—N bonds to result in ring opening and H-migration. An AIMD study on the initial chemical events in thermal decomposition of nitramine explosive CL-20[12] pointed out that CL-20 has only one distinct initial reaction channel (the N—NO_2 bond hemolysis) during unimolecular decompositions. It did not observe any HONO elimination reaction, whereas the ring-breaking reaction was followed by the NO_2 fission. Xue et al.[13] researched that the ring opening is observed to trigger molecular decay at all four shock conditions; while the sufficient NO_2 fission is observed at shock velocities (U_s)= 8 km·s^{-1} and 9 km·s^{-1}, and strongly inhibited at shock velocities (U_s=10 km·s^{-1} and 11 km·s^{-1}. There is obvious difference among the three researches, so it is necessary to study the initial and subsequent decomposition mechanisms of CL-20 under extreme conditions further.

In this work, we performed AIMD simulations to investigate initial decomposition mechanisms and subsequent decom-

Received Date: 2017-09-28; **Revised Date**: 2017-11-15

Project Supported: The NSAF Foundation of National Natural Science Foundation of China and China Academy of Engineering Physics(U1530104) and the Science Challenging Program

Biography: XIANG Dong(1988-), female, doctoral candidate, molecular simulation and computational materials. e-mail: 2247704093@qq.com

Corresponding Author: ZHU Wei-hua(1969-), male, professor, molecular simulation and computational materials. e-mail: zhuwh@njust.edu.cn

position process for crystalline CL-20 at extreme conditions (3000 K and 3000 K coupled with 44.5 GPa). These conditions were considered because 44.5 GPa is the initial decomposition pressure of CL-20 and its combustion flame temperature is 3000 K. Our purpose is to analyze its decomposition mechanisms under extreme conditions in detail and discuss the similarities and differences.

2 Simulations and Computational Method

Our AIMD simulations were performed within the framework of density functional theory[14-15] based on CASTEP code[16] using norm-conserving pseudopotentials[17] and a plane-wave expansion of the wave functions. The Perdew-Burke-Ernzerhof[18] (PBE) exchange-correlation function was employed. A kinetic energy cutoff of 500 eV for the plane wave expansions was used in the MD simulations and 750 eV for structural optimization calculating total energy calculations To correct DFT for the missing van der Waals (vdW) interaction, we used the Grimme (G06)[19] and Tkatchenko and Scheffler (TS)[20] corrections to the PBE functional. We controlled the ionic temperature and pressure using a Nose′ thermostat[21] and an Andersen barostat[22], respectively. A time step of 1.0 fs was used in time integration. Previous studies[23] reported that a time step of 1.2 fs was used to study the thermal decomposition of PETN. Reciprocal space was sampled using the G-centered Monkhorst-Pack scheme and only the gamma point was used for the simulations. The convergence criteria were 1×10^{-5} eV energy differences for solving the electronic wave function and 1×10^{-3} eV force for structural optimization difference for AIMD simulation. Both the NVT and NPT ensembles were employed.

The procedure for the AIMD simulations was as follows: First, the system was equilibrated at 298.15 K for 5 ps using NVT. Then, based on this equilibrated system, AIMD simulations were carried out using NVT at 3000 K and using NPT at 3000 K coupled with 44.5 GPa, respectively. The pressure was applied equally in all directions without any symmetry constraint. The simulation time for the AIMD simulations was set to 40 ps using NVT and 17 ps using NPT.

3 Results and Discussion

Before carrying out the calculations, we applied three different functionals (PBE-TS, PBE-G06, PBE) to relax the bulk CL-20 at ambient pressure without any constraint. Table 1 lists the relaxed and experimental cell parameters of CL-20. It is found that the calculation errors of a, b, c, β, and cell volume by the PBE-TS are −1.73%, −2.15%, −2.49%, 0.26%, and −6.65%, compared with the experimental results. The predicted errors by PBE-G06 are −1.16%, −1.56%, −1.03%, 0.004%, and −3.79%, respectively. The computation errors by the PBE are −7.58%, −7.1%, −6.39%, −0.29%, and −22.38%, respectively. This indicates that the lattice parameters estimated by the PBE-G06 are much closer to the experimental values than by the PBE-TS and PBE. Therefore, PBE-G06 was adopted for subsequent simulations.

Table 1 Comparison of relaxed lattice parameters of CL-20 with experimental data at ambient conditions

method	a /Å	b /Å	c /Å	β /(°)	cell volume /Å^3
Expt.	8.85	12.56	13.39	106.82	1424.15
PBE-TS	9.00 (−1.73)	12.83 (−2.15)	13.72 (−2.49)	106.55 (0.26)	1518.81 (−6.65)
PBE-G06	8.95 (−1.16)	12.75 (−1.56)	13.52 (−1.03)	106.82 (0.004)	1478.16 (−3.79)
PBE	9.52 (−7.58)	13.45 (−7.1)	14.24 (−6.39)	107.13 (−0.29)	1742.82 (−22.38)

Note: Values in parentheses correspond to the percentage differences relative to the experimental data.

3.1 Initial Decomposition Mechanism

Scheme 1 presents the initial decomposition mechanism of the CL-20 crystal using NVT. It is found that the initial decomposition steps of the CL-20 molecule in the CL-20 crystal have two different paths: the C—C cleavage and the C—H bond breaking. The initial decomposition of the CL-20 crystal was triggered by the C—H cleavage using NVT. Scheme 2 presents the initial decomposition mechanisms of the CL-20 crystal using NPT. It is found that there are three kinds of initial decomposition mechanisms of the CL-20 molecules. This is much more complex than that using NVT. The initial decomposition steps of the CL-20 molecules in the crystal include above-mentioned C—C bond breaking, the C—N bond rupture, and the N—NO_2 bond cleavage. The probability of the N—NO_2 bond cleavage is much higher than that of other two reaction pathways. This indicates that the N—NO_2 bond is much more sensitive using NPT (3000 K coulped with 44.5 GPa) than using NVT (3000 K). However, the initial decomposition of the CL-20 crystal was triggered by the C—C cleavage using NPT. Therefore, the pressure makes the initial reactions of the CL-20 molecule much more complex. Under the two extreme conditions, we did not observe any HONO elimination reaction during unimolecular decomposition. Different unimolecular decomposition pathways for other cyclic nitramine explosives such as dimethylnitramine (DMNA)[24], RDX[25-28], and HMX[29-34], have been theoretically investigated. It was reported that there are the following three types of decomposition mechanisms: (1) the N—N bond homolytic cleavage accompanied by the elimination of the NO_2 group, (2) HONO elimination, and (3) ring-opening reactions. Our findings that the

initial decomposition steps of CL-20 are the C—N and N—NO_2 bond rupture were observed in the unimolecular decompositions of DMNA, RDX, and HMX[24-34]. Isayev et al.[12] pointed out that the initial step of unimolecular decomposition of CL-20 at high temperatures (1000-3000 K) is the N—NO_2 bond hemolysis. This is in agreement with our simulations.

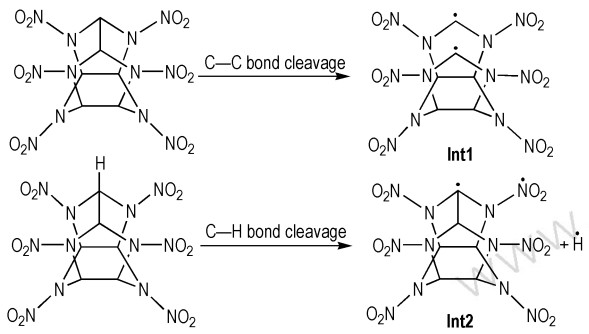

Scheme 1 Initial decomposition mechanisms of the CL-20 molecules in the crystal during the NVT simulation

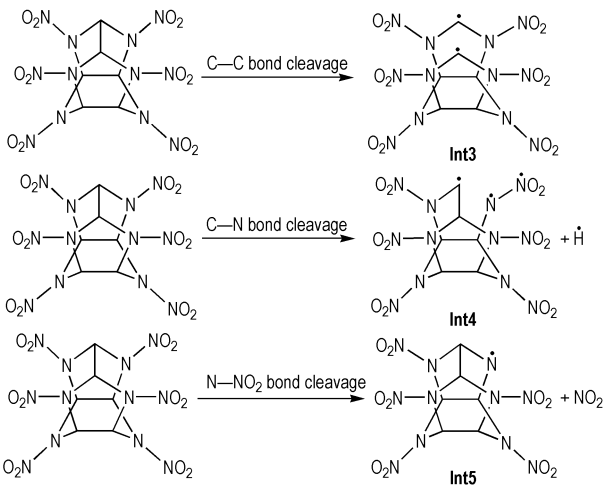

Scheme 2 Initial decomposition mechanisms of the CL-20 molecules in the crystal during the NPT simulation

3.2 Subsequent Decomposition Processes

More detailed subsequent decomposition processes after the initiation of the CL-20 crystal are shown in Scheme 3 and Scheme 4. It is seen in Scheme 3 that two major distinctive decomposition channels for the decomposition intermediates of CL-20 using NVT. These secondary reactions mainly include two interesting paths: Int1 produced Int1-1 by the breaking of N—NO_2 bond. Int1-2 decomposed by the C—N bond cleavage to produce two smaller fragments. This is the key step to produce the branch of the nine-membered heterocycles. After several reaction steps, it further produced the important fragment  . Int2 produced Int2-1 by the C—C bond breaking. Int2-1 further decomposed by the N—NO_2 bond breaking. The H atom attacked Int2 to produce Int2-2, which decomposed to produce Int2-3 by the C—C bond cleavage and the cage broke to form tricycle rings. The following reaction mainly released NO_2 to form  , which captured the oxygen atom form the NO_2 group and open the ring by the C—N bond cleavage.

It is found in Scheme 4 that there is only one major distinctive channel for secondary decomposition of the decomposition intermediates of CL-20 using NPT. The three intermediates INT3, INT4, and INT5 decomposed all through the N—NO_2 bond breaking to release NO_2. There are five N—NO_2 bonds breaking during the decomposition of INT3. After that, its cage structure collapsed by another C—C bond breaking to form INT3-2, which formed INT3-3 by the two C—N bond cleavage. This is the key step for the large ring breaking. There is an important intermediate of  with some branches produced during the decomposition. INT4-1 opened the C—N bond to form INT4-2, which produced the important intermediate of  with some branches by the cleavage of series of N—NO_2 bonds. INT5-1 decomposed by the breaking of the C—N and C—C bonds to form the important intermediate of  with some branches. After that, the tricycles are broken by the breaking of two C—N bonds to form INT5-3 fragment. This reaction is the same of the formation of INT1-3. However, INT5-3 became a tricycles form by the formation of a C—N bond again. Finally, INT5-4 is broken to form two five-membered heterocycles. Therefore, the decomposition reactions of the CL-20 crystal are sensitive to both high temperature and high pressure.

3.3 Decomposition Products

Fig. 1 shows the time evolution of the population of key products during the decomposition of the CL-20 crystal using NVT. The CL-20 crystal is decomposed quickly at the beginning during the simulation. The first N_2 is produced at the time of 800 fs. The concentration of N_2 increases step by step during the whole simulation time, reaching a relatively balance value of 14 molecules after t=10.05 ps. NO_2 is released quickly and its number reaches the maximum in a flash of reaction, but the number of NO_2 decreases when the products NO and OH produced. This indicates that some NO_2 decomposed to produce NO by capturing the H radicals to form OH fragment. Finally, NO_2 vanishes to form other products at about 5 ps. At the time point when the number of NO_2 reaches a maximum,

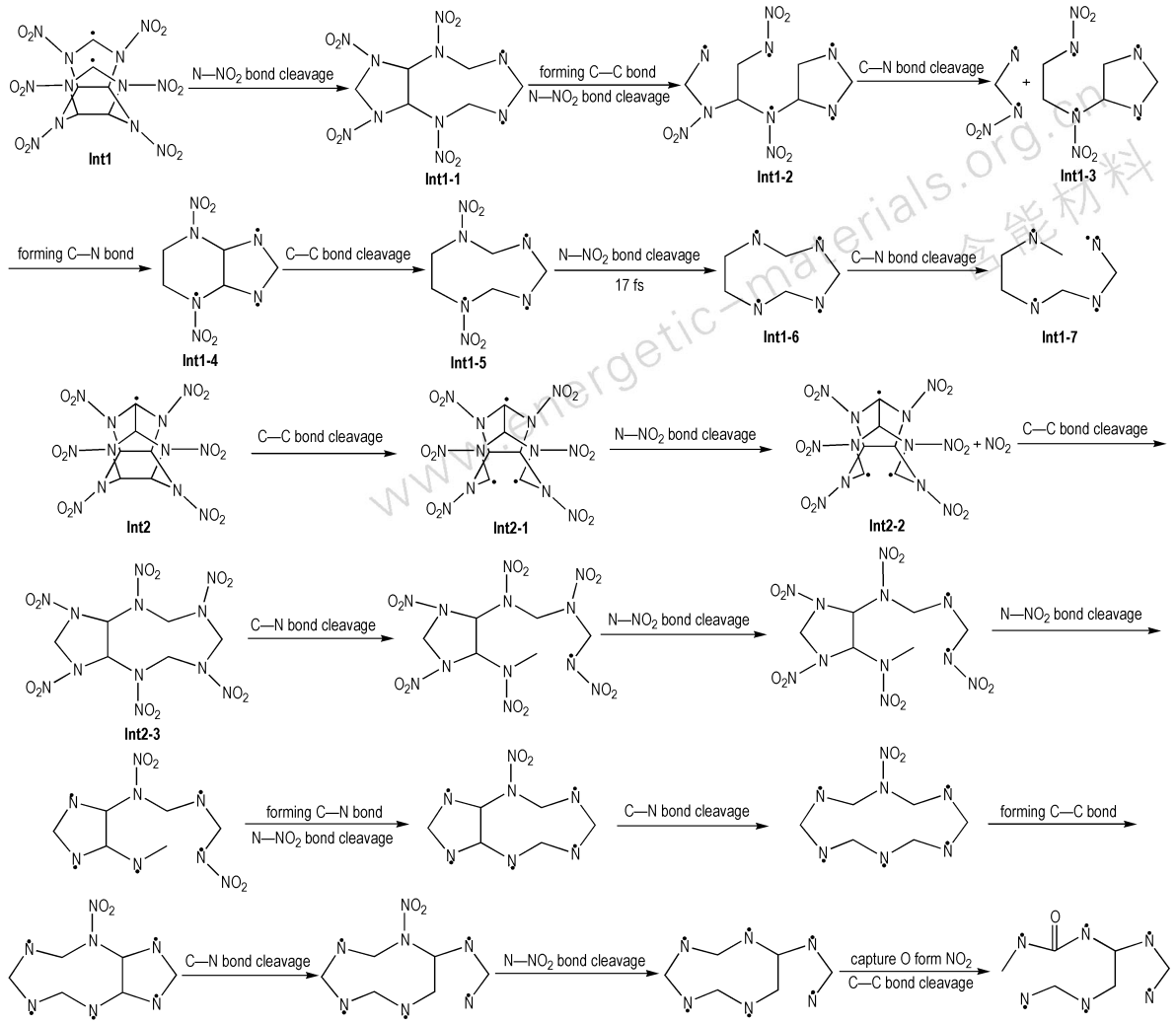

Scheme 3 Subsequent decomposition mechanisms of the CL-20 crystal during the NVT simulation

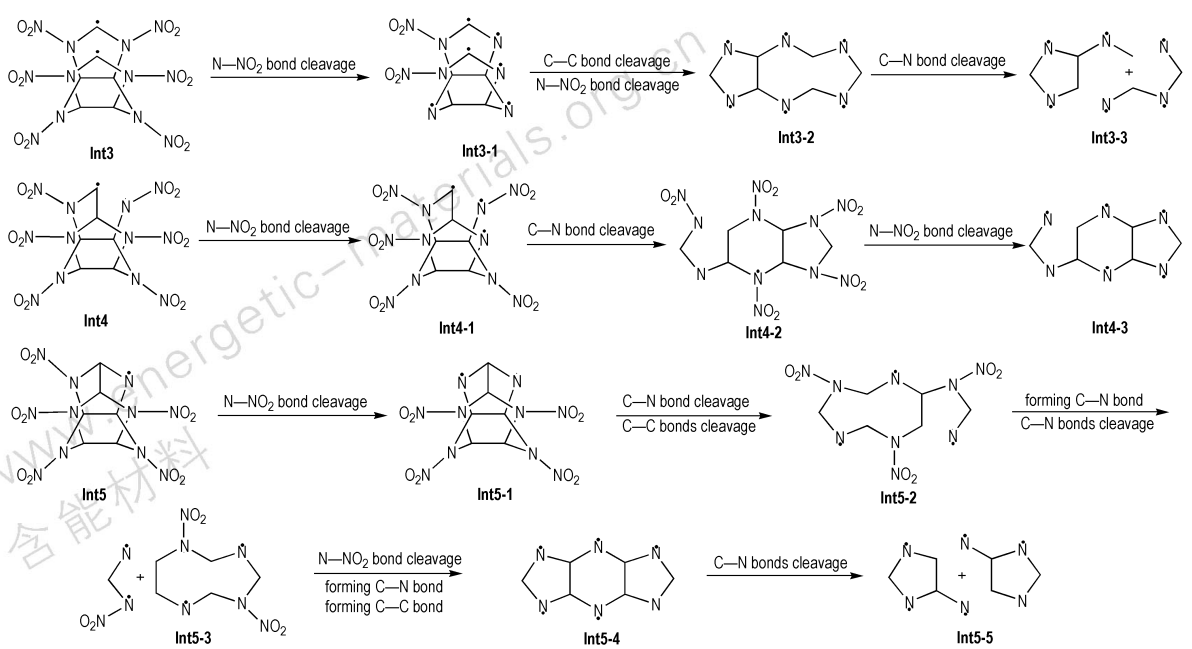

Scheme 4 Subsequence decomposition mechanisms of CL-20 during the NPT simulation

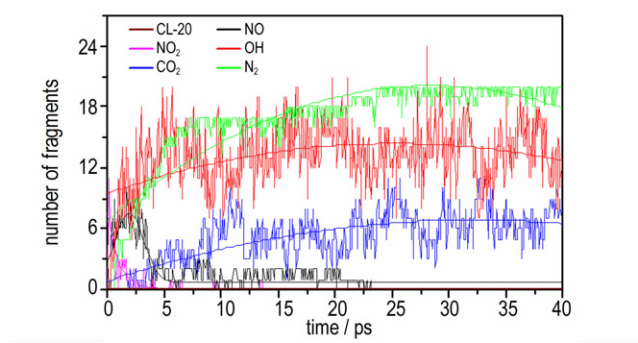

Fig.1 Time evolution of initial CL-20 molecules and products NO_2, CO_2, NO, OH, and N_2 during the NPT simulation

NO_2 is decomposed to produce NO. At 2.5 ps, the number of NO reaches the peak. NO diappears at about 23 ps. The number of OH has a similar variation trend with that of NO_2. According to the trendline of OH fragment, it can be deduced that the H radicals are very active. At about 1.55 ps, the first CO_2 is produced. Then the number of CO_2 increases and reaches a maximum of 10 at 10.05 ps. After that, a relative balance appears thereafter.

Fig.2 displays the time evolution of the population of key products during the decomposition of the CL-20 crystal using NPT. The number of main product N_2 increases gradually, reaching a relative balance value of 14 molecules at t=4.8 ps. Then it gets a balance thereafter. At the beginning of the decomposition, NO_2 increases quickly and reaches a maximum at about 0.5 ps. Then it decreases quickly but does not vanish during the whole reaction. NO increases accompanied by the decrease of NO_2 interestingly, it is seen in Fig.2 that the variation trend line for the number of OH keeps level during about 12 ps. This suggests that there is a balance between the formation and decay of OH at this extreme condition. At about 1 ps, CO_2 is produced and then increases, and reaches a balance, after about 10 ps. Although the main decomposition products are similar at these two extreme conditions, at the case of 3000 K coupled with 44.5 GPa is more complex than at 3000 K.

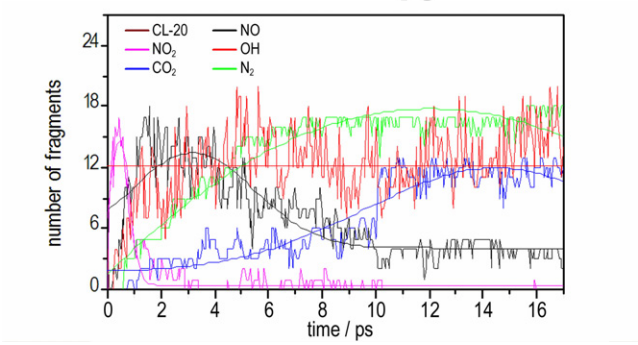

Fig.2 Time evolution of initial CL-20 molecules and products of NO_2, CO_2, NO, OH, and N_2 during the NPT simulation

Using NPT, one of important products is R-C_xO_y (x>2, y>5) during the decomposition of the CL-20 crystal. C_3O_6 clusters have attacked a new interest in the intense search for efficient, safe, and environment-friendly high energy density materials (HEDM), which can be used in propellants or explosives[35]. Fig.3 displays the total number of R-C_xO_y during the decomposition stage of the CL-20 crystal as a function of time at 3000 K coupled with 44.5 GPa. While the product R-C_xO_y has not been observed in the decomposition at 3000 K. This also shows that the decomposition is much more complex at 3000 K coupled with 44.5 GPa than at 3000 K. At about 7.5 ps, the number of R-C_xO_y reaches a maximum. The trendline of the number of R-C_xO_y is stable after 7.5 ps.

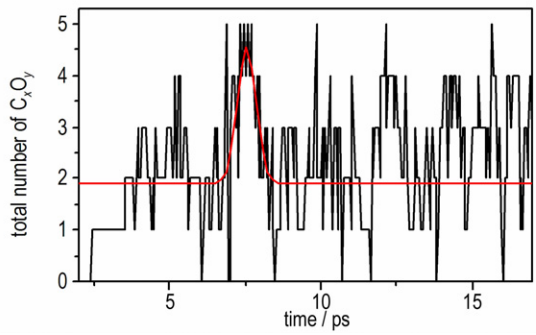

Fig.3 Time evolution of total number of the intermediate R-C_xO_y. The black thick trendline corresponds to the actual concentration data

Fig.4 compares the concentrations of the main decomposition products of the CL-20 crystal using NVT and using NPT as a function of time. It is found that the decomposition major products are the same using NVT and using NPT. The variation trends of the concentrations of corresponding main products are the same at two conditions. This obviously demonstrates that the decomposition mechanisms are sensitive to both the temperature and pressure. However, the concentrations of corresponding products using NPT are less than those using NVT. So the high pressure decelerates the decomposition.

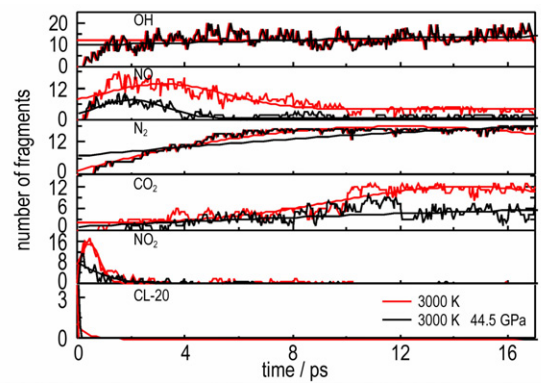

Fig.4 Comparison of time evolution of initial CL-20 molecules and products NO_2, CO_2, N_2, NO, and OH during the decomposition of the CL-20 crystal using NVT and using NPT. Red and black thick trend lines correspond to the actual concentration data using NVT and using NPT, respectively

4 Conclusions

In summary, we have performed AIMD simulations to understand the detailed and molecular-level information on the initial and following decomposition of high energy density material CL-20 under two extreme conditions. The results indicate that different reaction conditions led to different decomposition mechanisms of the CL-20 crystal.

(1) The initial decompositions of the CL-20 crystal using NVT and using NPT (3000 K and 3000 K coupled with 44.5 GPa) were triggered by the C—H cleavage and the C—C rupture, respectively. The subsequent decompositions mainly have two interesting paths using NVT and only one major distinctive channel using NPT. This indicates that the decomposition of the CL-20 crystal is sensitive to both high temperature and high pressure.

(2) The number of corresponding major products using NPT is smaller than those using NVT. This demonstrates that the high pressure decelerates the decomposition of CL-20.

Our theoretical studies provide a new insight into understanding coupling effects of the temperature and pressure on the initiation mechanisms and subsequent chemical decompositions of cage explosives.

References:

[1] Furman D, Kosloff R, Dubnikova F, et al. Decomposition of condensed phase energetic materials: interplay between uni- and bimolecular mechanisms[J]. *The Journal of the American Chemical Society*, 2014, 136(11): 4192-4200.

[2] Vagenknecht J A, Marecek P, Trzcinski W A. Sensitivity and performance properties of TEX explosives[J]. *The Journal of Energetic Materials*, 2002, 20(3): 245-253.

[3] Politzer P, Murray J S. Some perspectives on estimating detonation properties of C, H, N, O compounds[J]. *Central European Journal of Energetic Materials*, 2011, 8(3): 209-220.

[4] Koch E C. TEX-4,10-dinitro-2,6,8,12-tetraoxa-4,10-diazatetracyclo[5.5.0.05,9.03,11]-dodecane-review of a promising high density insensitive energetic material[J]. *Propellants, Explosives, Pyrotechnics*, 2015, 40(3): 374-387.

[5] Szecsody J E, Girvin D C, Devary B J, et al. Sorption and oxic degradation of the explosive CL-20 during transport in subsurface sediments[J]. *Chemosphere*, 2004, 56(6): 593-610.

[6] Iftimie R, Minary P, Tuckerman M E. Ab initio molecular dynamics: concepts, recent developments, and future trends[J]. *Proceedings of the National Academy of Sciences of the United States of America*, 2005, 102(19): 6654-6659.

[7] Wu Q, Zhu W H, Xiao H M. An ab initio molecular dynamics study of thermal decomposition of 3,6-di(azido)-1,2,4,5-tetrazine[J]. *Physical Chemistry Chemical Physics*, 2014, 16(39): 21620-21628.

[8] Ye C C, An Q, Goddard III W A, et al. Cis-1,3,4,6-tetranitrooctahydroimidazo-[4,5-d]imidazole] from quantum molecular dynamics simulations[J]. *The Journal of Physical Chemistry C*, 2015, 119(5): 2290-2296.

[9] Wu Q, Chen H, Xiong G L, et al. Decomposition of a 1,3,5-triamino-2,4,6-trinitrobenzene crystal at decomposition temperature coupled with different pressures: an ab initio molecular dynamics study[J]. *The Journal of Physical Chemistry C*, 2015, 119(29): 16500-16506.

[10] Wu Q, Xiong G L, Zhu W H, et al. How does low temperature coupled with different pressures affect initiation mechanisms and subsequent decompositions in nitramine explosive HMX? [J]. *Physical Chemistry Chemical Physics*, 2015, 17(35): 22823-22831.

[11] Okovytyy S, Kholod Y, Qasim M, et al. The mechanism of unimolecular decomposition of 2,4,6,8,10,12-hexanitro-2,4,6,8,10,12-hexaazaisowurtzitane. A computational DFT study[J]. *The Journal of Physical Chemistry A*, 2005, 109(12): 2964-2970.

[12] Isayev O, Gorb L, Qasim M et al. Ab initio molecular dynamics study on the initial chemical events in nitramines: thermal decomposition of CL-20[J]. *The Journal of Physical Chemistry B*, 2008, 112(35): 11005-11013.

[13] Xue X G, Wen Y S, Zhang C Y. Early decay mechanism of shocked εCL-20: A molecular dynamics simulation study[J]. *The Journal of Physical Chemistry C*, 2016, 120(38): 21169-21177.

[14] Kohn W, Sham L J. Self-consistent equations including exchange and correlation effects[J]. *Physical Review A*, 1965, 140(4): 1133-1138.

[15] Hohenberg P, Kohn W. Inhomogeneous electron gas[J]. *Physical Review Journals Archive* [*Sect.*] *B*, 1964, 136(3): 864-873.

[16] Segall M D, Lindan P J D, Probert M J, et al. First-principles simulation: ideas, illustrations and the CASTEP code[J]. *Journal of Physics: Condensed Matter*, 2002, 14(11): 2717-2744.

[17] Vanderbilt D. Soft self-consistent pseudopotentials in a generalized eigenvalue formalism[J]. *Physical Review B: Condensed Matter*, 1990, 41(11): 7892-7895.

[18] Perdew J P, Burke K, Ernzerhof M. Generalized gradient approximation made simple[J]. *Physical Review Letter*, 1996, 77(18): 3865-3868.

[19] Grimme S. Semiempirical GGA-type density functional constructed with a long-range dispersion correction[J]. *J Computational Chemistry*, 2006, 27(15): 1787-1799.

[20] Tkatchenko A, Scheffler M. Accurate molecular van der waals interactions from ground-state electron density and free-atom reference data[J]. *Physical Review Letter*, 2009, 102 (7): 073005-073009.

[21] Nosé S. A unified formulation of the constant temperature molecular dynamics methods[J]. *The Journal of Chemical Physics*, 1984, 81(1): 511-519.

[22] Andersen H C. Molecular dynamics simulations at constant pressure and/or temperature[J]. *The Journal of Chemical Physics*, 1980, 72(4): 2384-2393.

[23] Pozzo M, Davies C, Gubbins D, et al. Thermal and electrical conductivity of iron at earth's core conditions[J]. *Nature*, 2012, 485(7398): 355-358.

[24] Johnson M A, Truong T N. High-level ab initio and density functional theory evaluation of combustion reaction energetics: NO_2 and HONO elimination from dimethylnitramine[J]. *The Journal of Physical Chemistry A*, 1999, 103 (44): 8840-8846.

[25] Wu C J, Fried L E. Ab initio study of RDX decomposition mechanisms[J]. *The Journal of Physical Chemistry A*, 1997, 101(46): 8675-8679.
[26] Chakraborty D, Muller R P, Dasgupta S, et al. The mechanism for unimolecular decomposition of RDX (1,3,5-Trinitro-1,3,5-triazine), an ab initio study[J]. *The Journal of Physical Chemistry A*, 2000, 104(11): 2261-2272.
[27] Just C, Schnoor J. Phytophotolysis of hexahydro-1,3,5-trinitro-1,3,5-triazine(RDX) in leaves of reed canary grass[J]. *Environmental Science & Technology*, 2004, 38(1): 290-295.
[28] Long G T, Vyazovkin S, Brems B A, et al. Competitive vaporization and decomposition of liquid RDX[J]. *The Journal of Physical Chemistry B*, 2000, 104(11): 2570-2574.
[29] Chakraborty D, Muller R P, Dasgupta S, et al. Mechanism for unimolecular decomposition of HMX (1,3,5,7-tetranitro-1,3,5,7-tetrazocine), an ab Initio study[J]. *The Journal of Physical Chemistry A*, 2001, 105(8): 1302-1314.
[30] Zhang S, Truong T N. Thermal rate constants of the NO_2 fission reaction of gas phase α-HMX: a direct ab initio dynamics study [J]. *The Journal of Physical Chemistry A*, 2000, 104(31): 7304-7307.
[31] Zhang S, Truong T N. Branching ratio and pressure dependent rate constants of multichannel unimolecular decomposition of gas-phase α-HMX: an ab initio dynamics study[J]. *The Journal of Physical Chemistry A*, 2001, 105(11): 2427-2434.
[32] Zhang S, Nguyen H N, Truong T N. Theoretical study of mechanisms, thermodynamics, and kinetics of the decomposition of gas-phase α-HMX (octahydro-1,3,5,7-tetranitro-1,3,5,7-tetrazocine)[J]. *The Journal of Physical Chemistry A*, 2003, 107(16): 2981-2989.
[33] Lewis J P, Glaesemann K R, VanOpdorp K, et al. Ab initio calculations of reactive pathways for α-octahydro-1,3,5,7-tetranitro-1,3,5,7-tetrazocine (α-HMX)[J]. *The Journal of Physical Chemistry A*, 2000, 104(48): 11384-11389.
[34] Manaa M R, Fried L E, Melius C F, et al. Decomposition of HMX at extreme conditions: A molecular dynamics simulation [J]. *The Journal of Physical Chemistry A*, 2002, 106(39): 9024-9029.
[35] Zhang T, Zhang J M, Jiang H H, et al. A DFT study on the stable structures and dissociation mechanism of C_3O_6 cluster[J]. *Chinese Journal of Structural Chemistry*, 2011, 30(3): 443-447.

运用从头算动力学方法研究极端条件下 CL-20 的分解机理

向 东[1], 吴 琼[2], 朱卫华[1]
(1. 南京理工大学化工学院, 江苏 南京 210094; 2. 南京工程学院, 江苏 南京 211167)

摘 要: 运用从头算动力学方法研究一种高密度笼状化合物(CL-20)在极限条件下的分解机理。结果显示在不同的条件下,CL-20的起爆机理和分解过程都不相同,这表明 CL-20 对高温高压都很敏感。对比相应条件下主要产物的数量发现高压会抑制分解反应的进程。但是,在高压耦合高温时会生成 *R*-C_xO_y(x>2,y>5)中间体又意味着高压使分解反应更加复杂。在 *R*-C_xO_y(x>2, y>5)中间体中,化合物 C_3O_6 已经被证实是一种高能密度化合物。

关键词: 从头算分子动力学; 六硝基六氮杂异伍兹烷(CL-20); 分解; 极限条件
中图分类号: TJ55; O64 **文献标志码:** A **DOI:** 10.11943/j.issn.1006-9941.2018.01.007